Photic stimulation and spectral analysis

Light stimuli from a 100-W tungsten source were filtered (neutral density and narrow-band interference filters;10 nm width; Oriel), gated by a shutter (Uniblitz VS35;Vincent Associates) and calibrated by a radiometer (S370, UDT Instruments). The irradiance of the unfiltered ('white') stimulus was (in photons s^{-1} cm^{-2}): 4×10^{12} at 400 nm, 6×10^{13} at 500 nm and 1×10^{14} at 600 nm.

For spectral analysis, the culture medium contained 11-*cis*-retinaldehyde. Current injection held cells near −44 mV. Stable sensitivity, confirmed by retesting with a standard stimulus, required long interstimulus intervals (7 min). Stimuli of 480 nm were interleaved with those of two to three other wavelengths (420, 440, 540, 570 or 600 nm). Each response to one of these other wavelengths yielded an estimate of relative sensitivity normalized to that at 480 nm (see Fig. 4a), and these were averaged for each wavelength. For each cell, we determined the retinaldehyde template function[24] that best fitted these data (least-squares method). The two free parameters for the fit were λ_{max} and the vertical offset. Relative sensitivities were then re-normalized to that at the theoretical optimum (λ_{max}).

Calcium imaging

Cells loaded with the long-wavelength Ca^{2+} indicator Rhod-2-AM (4–6 μM in Tyrodes, 30 min, 37 °C) were imaged at 30 Hz using green excitation (525–550 nm; emission 580–650 nm; Chroma 31002a) attenuated 128- to 512-fold by neutral density filters. Integration time was fixed within trials (typically 32 frames) to optimize sensitivity and avoid saturation. Responses, analysed by ImageJ software (W. Rasband; http://rsb.info.nih.gov/ij/; 2004), were expressed as post-stimulus change in fluorescence intensity above baseline divided by the baseline intensity ($\Delta F/F$).

Further methodological details are provided in the Supplementary Methods.

Received 5 November 2004; accepted 10 January 2005; doi:10.1038/nature03345.
Published online 26 January 2005.

1. Provencio, I., Jiang, G., De Grip, W. J., Hayes, W. P. & Rollag, M. D. Melanopsin: An opsin in melanophores, brain, and eye. *Proc. Natl Acad. Sci. USA* **95,** 340–345 (1998).
2. Provencio, I. *et al.* A novel human opsin in the inner retina. *J. Neurosci.* **20,** 600–605 (2000).
3. Bellingham, J., Whitmore, D., Philp, A. R., Wells, D. J. & Foster, R. G. Zebrafish melanopsin: isolation, tissue localisation and phylogenetic position. *Brain Res. Mol. Brain Res.* **107,** 128–136 (2002).
4. Hannibal, J. & Fahrenkrug, J. Melanopsin: a novel photopigment involved in the photoentrainment of the brain's biological clock? *Ann. Med.* **34,** 401–407 (2002).
5. Hannibal, J., Hindersson, P., Knudsen, S. M., Georg, B. & Fahrenkrug, J. The photopigment melanopsin is exclusively present in pituitary adenylate cyclase-activating polypeptide-containing retinal ganglion cells of the retinohypothalamic tract. *J. Neurosci.* **22** RC191 (2002).
6. Hattar, S., Liao, H. W., Takao, M., Berson, D. M. & Yau, K. W. Melanopsin-containing retinal ganglion cells: architecture, projections, and intrinsic photosensitivity. *Science* **295,** 1065–1070 (2002).
7. Provencio, I., Rollag, M. D. & Castrucci, A. M. Photoreceptive net in the mammalian retina. *Nature* **415,** 493 (2002).
8. Berson, D. M. Strange vision: ganglion cells as circadian photoreceptors. *Trends Neurosci.* **26,** 314–320 (2003).
9. Gooley, J. J., Lu, J., Chou, T. C., Scammell, T. E. & Saper, C. B. Melanopsin in cells of origin of the retinohypothalamic tract. *Nature Neurosci.* **4,** 1165 (2001).
10. Berson, D. M., Dunn, F. A. & Takao, M. Phototransduction by retinal ganglion cells that set the circadian clock. *Science* **295,** 1070–1073 (2002).
11. Panda, S. *et al.* Melanopsin (Opn4) requirement for normal light-induced circadian phase shifting. *Science* **298,** 2213–2216 (2002).
12. Ruby, N. F. *et al.* Role of melanopsin in circadian responses to light. *Science* **298,** 2211–2213 (2002).
13. Lucas, R. J. *et al.* Diminished pupillary light reflex at high irradiances in melanopsin-knockout mice. *Science* **299,** 245–247 (2003).
14. Panda, S. *et al.* Melanopsin is required for non-image-forming photic responses in blind mice. *Science* **301,** 525–527 (2003).
15. Warren, E. J., Allen, C. N., Brown, R. L. & Robinson, D. W. Intrinsic light responses of retinal ganglion cells projecting to the circadian system. *Eur. J. Neurosci.* **17,** 1727–1735 (2003).
16. Lucas, R. J., Douglas, R. H. & Foster, R. G. Characterization of an ocular photopigment capable of driving pupillary constriction in mice. *Nature Neurosci.* **4,** 621–626 (2001).
17. Hattar, S. *et al.* Melanopsin and rod-cone photoreceptive systems account for all major accessory visual functions in mice. *Nature* **424,** 76–81 (2003).
18. Gooley, J. J., Lu, J., Fischer, D. & Saper, C. B. A broad role for melanopsin in nonvisual photoreception. *J. Neurosci.* **23,** 7093–7106 (2003).
19. Newman, L. A., Walker, M. T., Brown, R. L., Cronin, T. W. & Robinson, P. R. Melanopsin forms a functional short-wavelength photopigment. *Biochemistry* **42,** 12734–12738 (2003).
20. Bellingham, J. & Foster, R. G. Opsins and mammalian photoentrainment. *Cell Tissue Res.* **309,** 57–71 (2002).
21. Hurst, R. S., Zhu, X., Boulay, G., Birnbaumer, L. & Stefani, E. Ionic currents underlying HTRP3 mediated agonist-dependent Ca^{2+} influx in stably transfected HEK293 cells. *FEBS Lett.* **422,** 333–338 (1998).
22. Belenky, M. A., Smeraski, C. A., Provencio, I., Sollars, P. J. & Pickard, G. E. Melanopsin retinal ganglion cells receive bipolar and amacrine cell synapses. *J. Comp. Neurol.* **460,** 380–393 (2003).
23. Fields, T. A. & Casey, P. J. Signalling functions and biochemical properties of pertussis toxin-resistant G-proteins. *Biochem. J.* **321,** 561–571 (1997).
24. Lamb, T. D. Photoreceptor spectral sensitivities: common shape in the long- wavelength region. *Vision Res.* **35,** 3083–3091 (1995).
25. Rollag, M. D., Provencio, I., Sugden, D. & Green, C. B. Cultured amphibian melanophores: a model system to study melanopsin photobiology. *Methods Enzymol.* **316,** 291–309 (2000).
26. Yoshimura, T. & Ebihara, S. Spectral sensitivity of photoreceptors mediating phase-shifts of circadian rhythms in retinally degenerate CBA/J (rd/rd) and normal CBA/N (+/+)mice. *J. Comp. Physiol.* **178,** 797–802 (1996).
27. Brueggemann, L. I. & Sullivan, J. M. HEK293S cells have functional retinoid processing machinery. *J. Gen. Physiol.* **119,** 593–612 (2002).
28. Wong, S. K. G protein selectivity is regulated by multiple intracellular regions of GPCRs. *Neurosignals* **12,** 1–12 (2003).
29. Oh, E. J., Gover, T. D., Cordoba-Rodriguez, R. & Weinreich, D. Substance P evokes cation currents through TRP channels in HEK293 cells. *J. Neurophysiol.* **90,** 2069–2073 (2003).
30. Hardie, R. C. Regulation of TRP channels via lipid second messengers. *Annu. Rev. Physiol.* **65,** 735–759 (2003).
31. Melyan, Z., Tarttelin, E. E., Bellingham, J., Lucas, R. J. & Hankins, M. W. Addition of human melanopsin renders mammalian cells photoresponsive. *Nature* doi:10.1038/nature03344 (this issue).
32. Panda, S. *et al.* Illumination of the melanopsin signaling pathway. *Science* **307,** 600–604 (2005).
33. Isoldi, M. C., Rollag, M. D., de Lauro Castrucci, A. M. & Provencio, I. Rhabdomeric phototransduction initiated by the vertebrate photopigment melanopsin. *Proc. Natl Acad. Sci. USA* **102**(4), 1217–1221 (2005).

Supplementary Information accompanies the paper on **www.nature.com/nature**.

Acknowledgements We thank V. Maine for technical support; M. Zhu for donating the HEK293-TRPC3 cells; T. Helton, K. Richard, D. Lipscombe, J. Bai and X. Wang for guidance with cell culture; E. Newman and D. O'Malley for advice on calcium imaging; and M. Rollag and J. McIlwain for discussions and comments on the manuscript. This work was supported by NIH grants to D.M.B. and I.P.

Competing interests statement The authors declare that they have no competing financial interests.

Correspondence and requests for materials should be addressed to D.B. (David_Berson@brown.edu).

Melanopsin-expressing ganglion cells in primate retina signal colour and irradiance and project to the LGN

Dennis M. Dacey[1], Hsi-Wen Liao[2], Beth B. Peterson[1], Farrel R. Robinson[1], Vivianne C. Smith[3], Joel Pokorny[3], King-Wai Yau[2] & Paul D. Gamlin[4]

[1]*University of Washington, Dept of Biological Structure and the Washington National Primate Research Center, Seattle, Washington 98195-7420, USA*
[2]*Departments of Neuroscience and Ophthalmology, Johns Hopkins University School of Medicine, Baltimore, Maryland 21205-2185, USA*
[3]*University of Chicago, Vision Science Laboratories, 940 East 57th Street, Chicago, Illinois 60637, USA*
[4]*University of Alabama at Birmingham, Vision Science Research Center, Birmingham, Alabama 35294-4390, USA*

Human vision starts with the activation of rod photoreceptors in dim light and short (S)-, medium (M)-, and long (L)- wavelength-sensitive cone photoreceptors in daylight. Recently a parallel, non-rod, non-cone photoreceptive pathway, arising from a population of retinal ganglion cells, was discovered in nocturnal rodents[1]. These ganglion cells express the putative photopigment melanopsin and by signalling gross changes in light intensity serve the subconscious, 'non-image-forming' functions of circadian photoentrainment and pupil constriction[1–7]. Here we show an anatomically distinct population of 'giant', melanopsin-expressing ganglion cells in the primate retina that, in addition to being intrinsically photosensitive, are strongly activated by rods and cones, and display a rare, S-Off, (L + M)-On type of colour-opponent receptive field. The intrinsic, rod and (L + M) cone-derived light responses combine in these giant cells to signal irradiance over the full dynamic range of human vision. In accordance with cone-based colour opponency, the giant cells project to the lateral geniculate nucleus, the thalamic relay to primary visual cortex. Thus, in the diurnal trichromatic primate, 'non-image-forming' and conventional 'image-forming' retinal

pathways are merged, and the melanopsin-based signal might contribute to conscious visual perception.

There is evidence that a melanopsin-associated photodetective pathway exists in the diurnal human visual system[8–12], similar to the one found in the nocturnal rodent. However, the detailed anatomical and functional properties of a melanopsin pathway in primates, and its relationship to rod and cone circuits, are unknown. To identify the melanopsin-expressing cells in the primate, a polyclonal antibody derived from the conceptually translated, full-length complementary DNA for the human melanopsin protein was used to immunostain human and macaque retinae. In flat mounts of the entire retina, the melanopsin antisera revealed a morphologically distinct population of ~3,000 retinal ganglion cells with completely stained cell bodies, dendritic trees and axons (Fig. 1a–c). With ~1.5 million ganglion cells in the human retina, the melanopsin-expressing cells comprise only 0.2% of the total. The melanopsin-expressing ganglion cell bodies were big, giving rise to the largest dendritic tree diameters of any primate retinal ganglion cell identified thus far[13] (Fig. 1d–f). The long, sparsely branching dendrites produced an extensive meshwork of highly overlapping processes. Cell counts showed a shallow density gradient ranging from 3–5 cells mm^{-2} over much of the retinal periphery to a peak of 20–25 cells mm^{-2} in the parafoveal retina (Fig. 1g); in contrast, total ganglion cells reach a peak density of ~50,000 cells mm^{-2}. In the central retina, the extremely large dendritic trees of melanopsin-containing ganglion cells spiralled around the foveal pit to form an extensive plexus (Fig. 1e). Melanopsin-containing dendrites were localized to two strata: the extreme inner and extreme outer borders of the inner plexiform layer (Fig. 1h). Individual cells are principally monostratified, creating two distinct subpopulations that send dendrites to either the inner or the outer stratum. About 60% of the melanopsin-expressing cells were outer-stratifying cells, and about 40% had cell bodies displaced to the inner nuclear layer

A novel cell-marking method was used in conjunction with the *in vitro* intact macaque retina[14] to investigate the central targets and the visual physiology of the melanopsin-expressing cells. The tracer rhodamine dextran was injected into physiologically identified locations in the lateral geniculate nucleus (LGN) and pretectal olivary nucleus (PON), two major retinorecipient structures. After retrograde transport, the complete dendritic morphology of labelled ganglion cells was revealed in the *in vitro* retina by liberation of the sequestered rhodamine tracer into the cytoplasm upon light exposure[13]. Melanopsin immunostaining always colocalized with rhodamine in the cell body and dendritic tree of the tracer-labelled 'giant' cells (Fig. 2a–d). These distinctive 'giant', monostratified ganglion cells appear identical to those previously labelled in a similar retrograde fashion from both LGN and PON[13].

The giant ganglion cells showed cone-driven input and an unexpected response to chromatic stimuli. At mid-photopic levels, a 550-nm light pulse evoked a sustained On response (Fig. 3a). Latencies to first spike were ~30–40 ms, typical of cone-mediated ganglion cell signals in primates (Fig. 3a inset). Surprisingly, a sustained On response was observed for both morphological cell

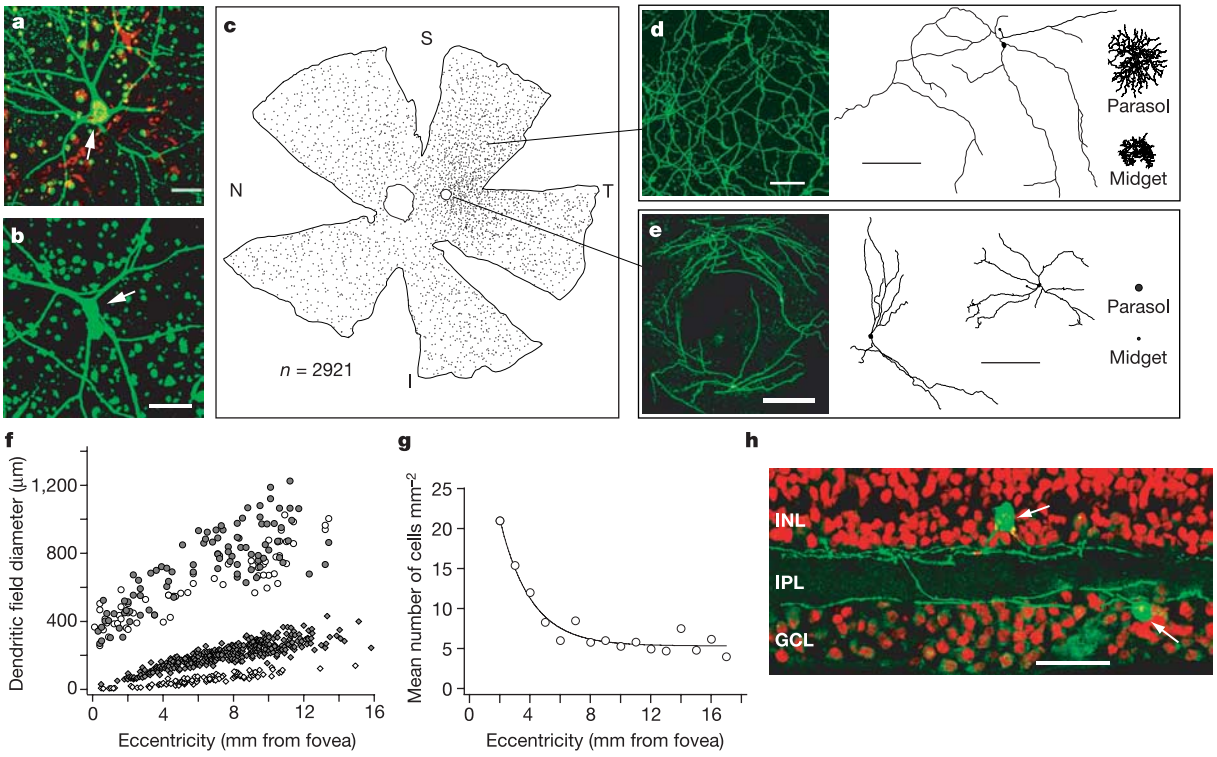

Figure 1 Morphology of melanopsin-immunoreactive cells. **a**, Human cell (arrow); propidium iodide red counterstain. Scale bar, 50 μm. **b**, Macaque cell (arrow). Scale bar, 50 μm. **c**, Macaque retina tracing; dots represent melanopsin cells. T, temporal retina; N, nasal retina; S, superior retina; I, inferior retina. **d**, Melanopsin cells in peripheral retina (left; scale bar,100 μm). Tracing of a peripheral HRP-stained giant cell (right; scale bar, 200 μm). Parasol and midget cells (far right) are shown for comparison. **e**, Melanopsin cells encircling the fovea (left; scale bar, 200 μm). Tracings of two HRP-stained giant cells ~1–1.5 mm from the fovea (right; scale bar, 200 μm). Circles (far right) indicate size of foveal parasol and midget cells. **f**, Dendritic field size of melanopsin cells versus eccentricity (inner cells, filled circles, $n = 93$; outer cells, open circles, $n = 63$). Parasol (filled diamonds, $n = 333$) and midget cells (open diamonds, $n = 93$) are shown for comparison. **g**, Mean cell density of melanopsin cells versus eccentricity (total 614 cells in 78 1 mm^2 samples). **h**, Dendritic arbours (green) of melanopsin cells (arrows) from stacked confocal images of 5 consecutive vertical sections (25 μm thick). The soma of the outer cell is displaced to the inner nuclear layer (INL). GCL, ganglion cell layer; IPL, inner plexiform layer. Scale bar, 50 μm.

populations (Fig. 3a), showing that the inner-versus-outer stratification, normally reflecting a division into On-centre versus Off-centre receptive field categories, does not apply here. Furthermore, these cells showed an unusual 'colour-opponent' receptive field in which an S cone-mediated Off response is antagonistic to an (L + M) cone-mediated On response (Fig. 3b). Cone-mediated receptive fields were large, approximating the dendritic tree diameter, and they showed spatially overlapping S-Off and (L + M)-On components, with little evidence of the strong inhibitory-surround typical of primate ganglion cells that project to the LGN (Fig. 3b, middle inset).

When the *in vitro* retina was maintained in total darkness for 10–20 min, light stimuli in the scotopic range elicited strong rod-driven responses (Fig. 3c). The response was a sustained On-type with the long latency to spike (~150 ms) (Fig. 3c, inset) and spectral tuning (peak at 502 nm, data not shown) characteristic of rod-driven input. The rod signal showed high photosensitivity, responding to quantal illuminances as low as 6–7 log quanta $cm^{-12}\,s^{-1}$ (or 4–5 log units below the threshold for a cone-mediated response), which is at or near the absolute threshold for human vision[15].

Intrinsic photosensitivity was unmasked in the giant ganglion cells by pharmacologically blocking rod and cone transmission to the inner retina. Bath application of L-AP4 (DL-2-amino-4-phosphono-butyric acid) and CNQX (6-cyano-7-nitroquinoxaline-2,3-dione), which block both ionotropic and metabotropic

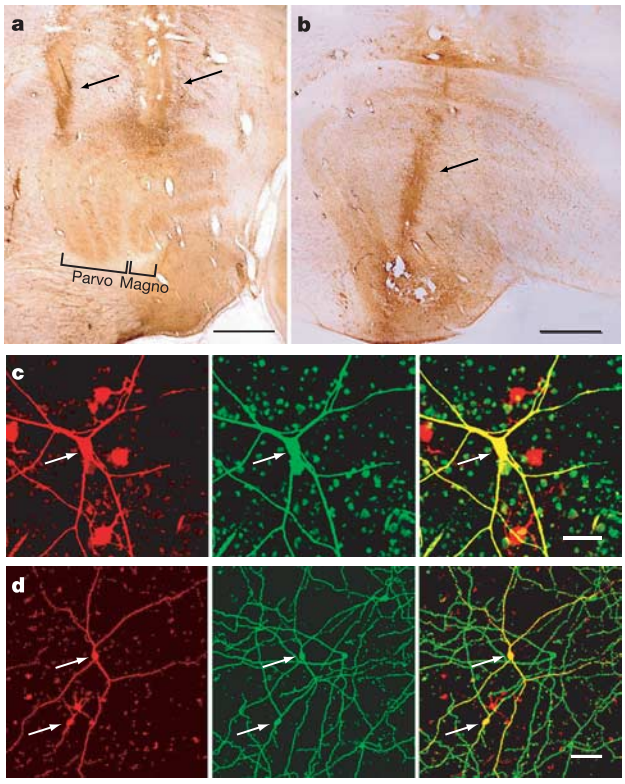

Figure 2 Retrograde tracer labelling from LGN and pretectum colocalize with melanopsin immunostain. **a**, **b**, Coronal sections through LGN showing HRP-stained tracer injection tracks (arrows). Injections in **a** are restricted to the parvocellular layers; the track in **b** extends to the magnocellular layers. Scale bars, 2 mm. **c**, Confocal images of retrograde rhodamine (red) labelling (left, arrow) from LGN injection and melanopsin (green) immunostaining (middle, arrow). Colocalization of labels appears yellow (right, arrow). Scale bar, 50 μm. **d**, Cells retrogradely labelled with rhodamine from pretectum injections (left, arrows) and melanopsin-immunostained (middle, arrows). Colocalization appears yellow (right, arrows). Scale bar, 100 μm.

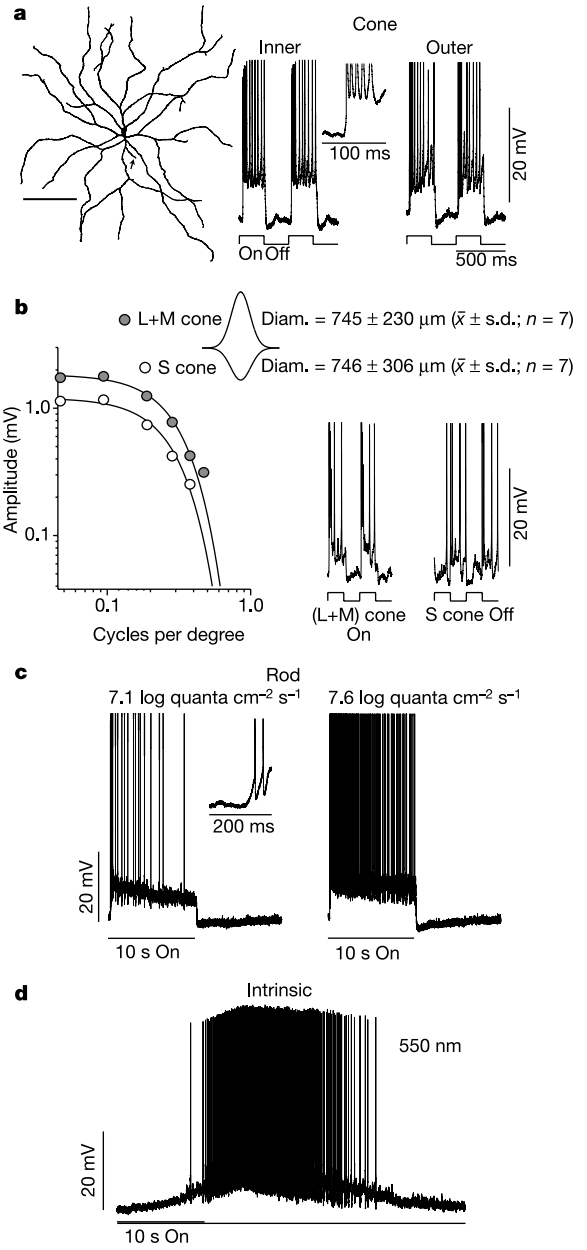

Figure 3 Giant cells show rod and colour-opponent inputs and are inherently photoreceptive. **a**, Tracing of a giant cell (arrow indicates axon; scale bar, 200 μm). The cell was recorded from and intracellularly filled with Neurobiotin in the *in vitro* retina. Voltage traces (right) show sustained On responses of an inner and an outer cell to a 2-Hz modulated 550-nm, full-field monochromatic light (13.5 log quanta $cm^{-2}\,s^{-1}$) under photopic conditions. Inset: first 100 ms of voltage response of inner cell; response latency is 38 ms. Stimulus time indicated below voltage traces. **b**, The cell had an (L + M)-On, S-Off opponent receptive field. Plot (left) shows spatial frequency response to drifting gratings used to measure the receptive field; stimuli modulated the L + M cones (dark grey circles) or S cones (white circles) in isolation. Data were fitted with a difference-of-gaussians receptive field model (solid lines). Two-dimensional gaussian profile (middle) summarizes fits for 7 cells. Traces (far right) show responses to (L + M) and S cone-isolating stimuli, respectively. **c**, Pure rod-mediated responses elicited by a 550-nm monochromatic pulse at low scotopic levels. Inset: first 200 ms of voltage response at 7.1 log quanta $cm^{-2}\,s^{-1}$; response latency is 147 ms. **d**, L-AP4 and CNQX application block excitatory glutamatergic transmission, revealing a slow, sustained, inherent photoresponse (550-nm light; 13.5 log quanta $cm^{-2}\,s^{-1}$).

retinal glutamate receptors, completely eliminated the short-latency, cone-driven light response at photopic levels. However, long-duration light pulses still elicited a depolarizing voltage response that grew slowly and declined even more slowly after stimulus offset (Fig. 3d). This intrinsic photoresponse is much like that observed previously in melanopsin-expressing ganglion cells in rat under pharmacological blockade of all synaptic transmission[1,6]. The long latency and sustained depolarization of the isolated intrinsic response was not an artefact created by drug application to the *in vitro* retina, because the latency to first spike varied systematically with stimulus strength, speeding up significantly at higher light levels (Fig. 4c). Moreover, in the drug-free condition, the fast cone-mediated response latency[15] was observed in combination with the slow, sustained depolarization derived from the intrinsic response (Fig. 5d).

To investigate spectral tuning, we measured peak depolarization as a function of wavelength over a 3-log-unit illuminance range (Fig. 4a–c) to determine relative quantal sensitivity (Fig. 4d, e). These data were well-fitted by an A1 visual pigment nomogram with a peak at 482 nm (Fig. 4f, mean ± s.d., 482 ± 1 nm; $n = 5$ cells), and were therefore distinct from primate rod, S, M and L cone pigments.

The regular and tonic spiking behaviour of the inherent photoresponse linearly encodes quantal illumination over a 3–4-log-unit range that encompasses most of daylight vision in the natural environment. The precise photon-counting capability in the macaque giant cells can be shown by counting the total number of spikes elicited by a long-duration light pulse, including those after light offset (Fig. 5a). Mean spike rate also increases regularly with increasing irradiance (Fig. 5b). Thus, the inherent photoresponse, when isolated, appears to transmit a signal that best measures total retinal irradiance when accumulated over long time periods; this property could serve as a neural memory of long-term light history to be used by the circadian system[16].

How does the intrinsic photoresponse of the giant ganglion cells interact with the rod- and/or cone-mediated signals under physiological conditions? Irradiance coding is present in the dark-adapted, pure rod response (Fig. 5b) but is not normally associated with the cone signal[17]. Without pharmacological blockade of the cone input, it was possible to observe a summation of short-latency depolarizing cone response and slow intrinsic response over most of the photopic range at 470 nm (Fig. 5b, d). On the surface, the inherent response appears to simply elevate the cone-mediated spike rate and sustain the firing beyond the duration of light stimulus (Fig. 5d, e). In actuality, however, the inherent response serves to compensate for the relative transience of the cone signal. This interaction can be appreciated by comparing the (L + M) cone-mediated On response elicited by a long-wavelength light with the mixed cone/intrinsic response elicited by a short-wavelength light at about the same quantal level (Fig. 5f, g). The (L + M) cone-mediated response is transient at threshold (Fig. 5f, left) and, even at the highest photopic levels used in this study (Fig. 5f, right), declines rapidly during a maintained light step. In contrast, when a short-wavelength light is used, the depolarizing, intrinsic response is added, making the response at threshold more sustained and apparently masking any transient inhibition from S cones (Fig. 5g, left). At higher light levels the cone + intrinsic response shows characteristic continued discharge after light offset (Fig. 5g, right).

We have shown that some basic properties of the melanopsin pathway, such as the dynamics and spectral tuning of the inherent light response and a projection to the brainstem pupillomotor nucleus, are conserved from rodents to primates. However, our findings reveal a fundamental contribution of rod/cone signals to this circuit in the diurnal primate and at the same time provide the first evidence of a broader role for this pathway in higher visual processing. By combining the rod, cone and inherent photo-

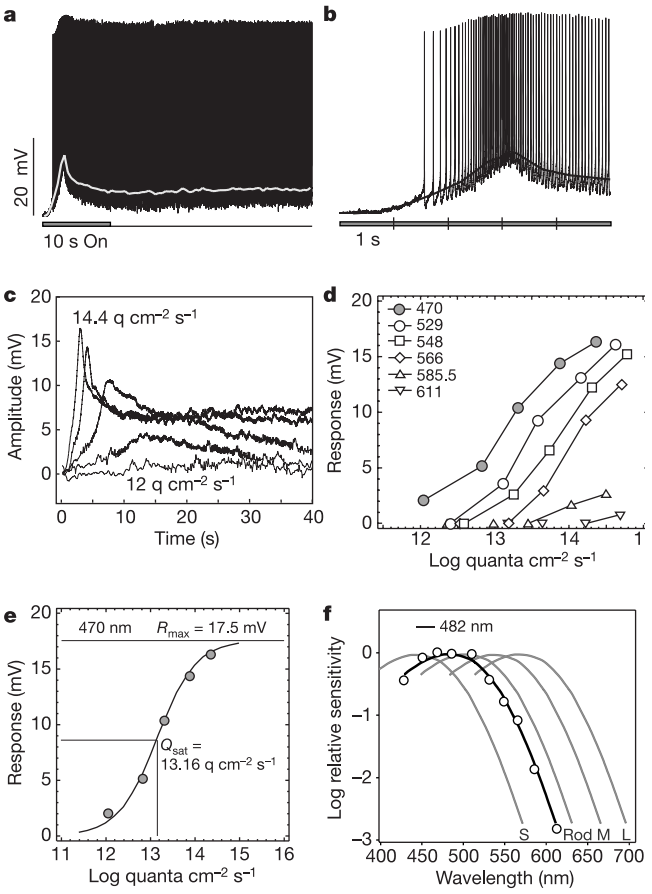

Figure 4 Spectral sensitivity of the giant cell's inherent light response. **a**, Response to a 470-nm pulse at 14.35 log quanta $cm^{-2}\,s^{-1}$ showed a peak of 40 impulses s^{-1} near 3 s, and continued firing for 30 s after the end of the light stimulus. White line shows membrane potential values averaged over 0.5 s sliding time windows. **b**, First 5 s of the response shown in **a**; averaged values pass near the spike initiation event. **c**, Averaged responses to 470-nm stimulus over a 12–14.5 quanta $cm^{-2}\,s^{-1}$ illuminance range; peak response was 16 mV for the brightest stimulus. **d**, Plot of averaged response peaks for 6 wavelengths between 470 and 611 nm as a function of quantal illumination. **e**, Michaelis–Menten equation fitted to the 470-nm data; responsivity was assessed for 10 wavelengths. **f**, Responsivity scaled for best fit to an A_1-based photopigment nomogram of 482 nm (solid line).

responses, the giant ganglion cell pathway can by itself convey signals from all receptor classes known to drive the circadian and pupillomotor systems[2,7]. Through chromatic opponency, the cone circuitry may have originally evolved to signal the large spectral changes at dawn and dusk to the circadian pathway in order to more precisely set the biological clock to the solar day[18]. Along the primary visual pathway, neurons with S-Off and S-On opponent receptive fields have been previously identified in the LGN[19] and primary visual cortex[20], and are basic components of psychophysical models of human colour vision[21]. S-On signals originate from at least two novel ganglion cell populations[13,14], but the origin of an S-Off signal has remained uncertain[22]. The giant cells demonstrate that S-Off, like S-On opponency, can also derive from a distinct ganglion cell population. Reciprocally, the sustained, irradiance-coding signal mediated by the intrinsic light response would presumably also reach primary visual cortex via the LGN. Over 30 years ago, Horace Barlow first called attention to a few exceptional 'luminance coding' units in the cat's retina, in which spike rate increased monotonically with increasing irradiance[23]. Similar

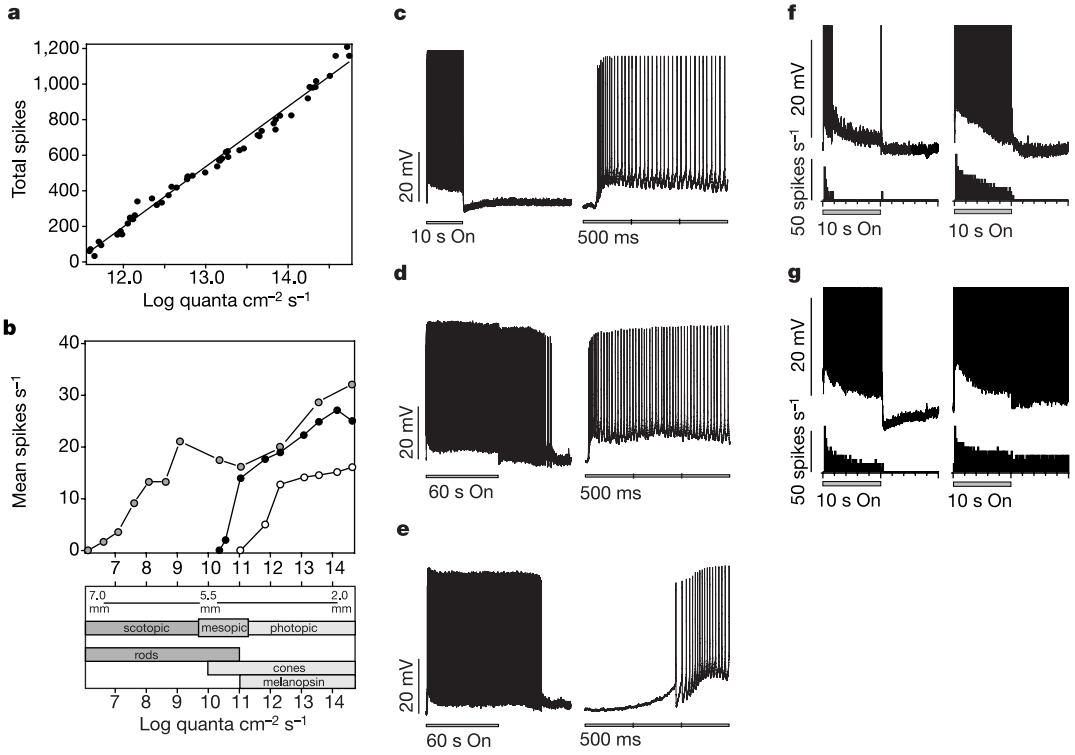

Figure 5 Irradiance coding and visual sensitivity range for the giant cell. **a**, Total spikes following a 10-s pulse for each wavelength used to measure spectral tuning (see Fig. 4), plotted versus log quanta $cm^{-2}\,s^{-1}$, weighted by the probability of absorption calculated from the OP^{482} nomogram (linear regression fit, $r = 0.99$, slope = 339 spikes per log unit). **b**, Response of a giant cell to a monochromatic light step (470 nm) as a function of retinal illuminance for 3 stimulus conditions: dark-adapted (grey circles), 10-s pulse after 20 min total darkness; light-adapted (black circles), 60-s pulse immediately after several min at high photopic levels (>14 quanta $cm^{-2}\,s^{-1}$); isolated intrinsic (open circles), 60-s pulse after light adaptation in the presence of bath-perfused L-AP4 and CNQX. Boxed area below plot shows melanopsin-associated (melanopsin) and rod and cone response ranges in relation to scotopic, mesopic, and photopic ranges of human vision and pupil diameter[15]. **c**–**e**, Intracellularly recorded light responses under the 3 conditions shown in **b**. **c**, Rod-mediated (dark-adapted) response at 8.1 log quanta $cm^{-2}\,s^{-1}$; latency to first spike, 147 ms. **d**, Cone-mediated (light-adapted) response at 13.5 log quanta $cm^{-2}\,s^{-1}$; latency, 36 ms. Prolonged spiking due to inherent photoresponse is seen at the end of the 60 s stimulus pulse. **e**, Inherent (isolated intrinsic) response at 13.5 log quanta $cm^{-2}\,s^{-1}$ after block of cone input; latency, 903 ms. **f**, Pure cone-mediated responses to 610-nm light pulse at both low (left; 12 log quanta $cm^{-2}\,s^{-1}$) and high (right; 15.2 log quanta $cm^{-2}\,s^{-1}$) photopic levels; post-stimulus time-spike histograms are below voltage traces. **g**, Summed cone and intrinsic response to 470-nm pulse at low (left; 11 log quanta $cm^{-2}\,s^{-1}$) and high (right; 14.6 log quanta $cm^{-2}\,s^{-1}$) photopic levels.

irradiance-coding units have been recorded in macaque LGN[24] and primary visual cortex[25], with a maintained discharge rate set by the overall level of diffuse illumination. The origin and spectral signature of this higher signal has yet to be determined, but it might arise from the giant cells described here and play a role in the conscious perception of brightness[26,27] □

Methods

All experimental procedures were approved by the Institutional Animal Care and Use Committees at either the University of Washington or the University of Alabama.

Antibody preparation

A peptide consisting of 19 amino acid residues, MNPPSGPRVPPSPTQEPSC, from the N terminus of the conceptually translated human melanopsin protein (NCBI accession number AAF24978) was synthesized (Princeton BioMolecules), with an additional lysine residue at the amino end for crosslinking. Purified peptide was crosslinked to thyroglobulin using glutaldehyde, then dialysed in PBS buffer. The peptide conjugate was used to immunize rabbits (Covance); the resulting antiserum was purified using peptide-bovine serum albumin (BSA)-packed affinity column.

Melanopsin immunostaining

Adult human and macaque retinae were fixed flat in 4% paraformaldehyde for 2 h, then washed in 0.1 M phosphate buffer (pH 7.4). Whole retinae were blocked in 0.1% Triton-X100 (Sigma) and 0.5% BSA in PBS for 3 h. The melanopsin antibody (1:100) was added and retinae were incubated for 4 days at 4 °C. After washing, macaque retinae were incubated in either biotinylated goat anti-rabbit antibody (BA-1000, Vector Labs) (8 animals) at 1:100 in 0.1% Triton-X100 and PBS for 48 h at 4 °C, or in Alexa Fluor 488 goat anti-rabbit antibody (A-11034, Molecular Probes)(1 animal) at 1:100 in PBS for 48 h at 4 °C. Human retinae were processed with the Alexa Fluor secondary antibody only. Retinae treated with biotinylated antibody were incubated in 0.1% Triton-X100 containing the Vector avidin-biotin-HRP complex (ABC Elite kit, Vector Labs) for 1–2 days at 4 °C, rinsed in phosphate buffer, and processed for HRP histochemistry by incubation in diaminobenzidine (DAB, 0.1% in 0.01 M phosphate buffer, pH 7.4) for 5 min, followed by addition of H_2O_2 (0.03%) and further incubation for 3–4 min. Frozen vertical sections (25 μm) of macaque retina were reacted using the same protocol except that primary antibody incubation was 10–12 h, secondary antibody incubation was 7–8 h, and avidin-biotin-HRP incubation was ~4–5 h. Sections were counterstained with the nuclear dye propidium iodide.

Cell counts

Melanopsin-immunostained cells were counted by taking sequential confocal images of all labelled cells, then 'splicing' the images together to reconstruct the entire retina. A grid was placed over the image of the reconstructed retina, centred on the fovea, and a small dot was placed over each fluorescent cell. The cells in each mm^2 of the grid were counted and the total number of labelled cells in the retina mapped.

Rhodamine-melanopsin colocalization

In two monkeys, biotinylated rhodamine dextran was used to retrogradely tracer-label retinal ganglion cells projecting to the LGN and pretectum, followed by melanopsin immunostaining of the retinae. Animals were anesthetized and prepared for recording in an aseptic surgery as described elsewhere[13]. In brief, the position of the LGN or pretectum was determined stereotaxically and evaluated by mapping extracellular responses to flashes of light. In each targeted area, ~0.5 μl injections were made of 10% biotinylated dextran-conjugated tetramethylrhodamine 3,000 MW (micro ruby, #D-7162, Molecular Probes) in sterile saline. After 4–7 days, the animal was deeply anesthetized, the eyes removed, and retinae prepared for the *in vitro* experiment. Animals were perfused through the heart with 800 ml warm (~37 °C) normal saline followed by 4 litres cold (~4 °C) 4% paraformaldehyde. Frozen brain sections were processed as described above for the retina,

to reveal biotin labelling at the injection sites. Rhodamine-labelled cells in the retina were visualized *in vitro* with a green filter block (excitation filter 545 nm, barrier filter 590 nm). The fluorescent label, initially confined to small bright spots in the soma and proximal dendrites, diffused throughout the entire dendritic tree after brief light exposure[13]. After the *in vitro* experiment, retinae were fixed and processed for melanopsin immunoreactivity as described above. Confocal images of rhodamine (red) and Alexa Fluor 488 (green) labelled cells were used to demonstrate colocalization.

In vitro preparation and intracellular recording

The *in vitro* retina preparation and recording have been described previously[14]. Eyes were removed from deeply anesthetized animals and the retina was isolated from the vitreous and sclera in oxygenated Ames' Medium (Sigma). The retina-RPE-choroid was placed flat, vitreal surface up, in a superfusion chamber mounted on the stage of a light microscope. Rhodamine-labelled cells were visualized as described above. Intracellular recording of targeted cells was done using high-impedance (~300–450 MΩ) glass micropipettes filled with 2–3% Neurobiotin (Vector Labs) and 1–2% pyranine (Molecular Probes) in 1.0 M potassium acetate. Voltage responses were amplified (Axoclamp, Axon Instruments) and digitized at 10 kHz.

Light stimulation

Square-wave pulses and sinusoidally-modulated stimuli were created using a VSG3-series stimulus generator (Cambridge Research Systems), which produced video input to a digital light projector (Vista Pro Plus, Christie Digital Systems). The projector output was relayed to the microscope camera port and focused on the retina by a microscope objective. A detailed description of the stimulator has been published[28]. Spectral opponency was evaluated with stimuli that modulated S-cones or (L + M) cones in isolation[29]. Drifting sinusoidal gratings (2 Hz temporal frequency) that modulated either the S-cones or the (L + M) cones in isolation but varied in spatial frequency were used to determine receptive field structure. Response amplitudes to a cone-isolating grating series were used to determine the parameters of a difference-of-gaussians receptive field model[30].

L-AP4 and CNQX application

A solution of 100 μM L-AP4 (Sigma) and 75 μM CNQX (Tocris) in oxygenated Ames' medium was applied to the retina. All cone-driven responses to temporally modulated square-wave stimuli (0.5–10 Hz) disappeared within 2–3 min of application. Drugs were superfused for up to 1–12 h during recordings of inherent light responses of giant cells ($n = 27$). Cone-mediated responses recovered within a few minutes of drug washout in all cases.

Spectral tuning

After pharmacological isolation of rod- and cone-mediated responses, a Varispec liquid crystal tuneable imaging filter inserted in the light path between projector and microscope was used to select narrow-band stimuli (15–20 half-bandwidth) at ten wavelengths (430–610 nm in 20-nm steps). Out-of-band light was minimized by selecting the suitable digital light projector primary for each of the wavelengths during stimulus presentation, and by setting the Varispec wavelength to 700 nm between stimulus presentations. The light stimulus was a 10-s pulse followed by 30 s recovery in the dark. At each wavelength, ganglion cell responses were measured at 0.5 log unit illuminance intervals from 10.5–14.5 log quanta $cm^{-2} s^{-1}$. Peak response was plotted as a function of quantal illumination; responsivity was assessed for each wavelength and fit to a visual pigment A_1 nomogram. Nomograms were scaled in 1-nm steps.

Received 21 September 2004; accepted 21 January 2005; doi:10.1038/nature03387.

1. Berson, D. M., Dunn, F. A. & Takao, M. Phototransduction by retinal ganglion cells that set the circadian clock. *Science* **295,** 1070–1073 (2002).
2. Hattar, S. *et al.* Melanopsin and rod-cone photoreceptive systems account for all major accessory visual functions in mice. *Nature* **424,** 75–81 (2003).
3. Lucas, R. J. *et al.* Diminished pupillary light reflex at high irradiances in melanopsin-knockout mice. *Science* **299,** 245–247 (2003).
4. Panda, S. *et al.* Melanopsin (Opn4) requirement for normal light-induced circadian phase shifting. *Science* **298,** 2213–2216 (2002).
5. Ruby, N. F. *et al.* Role of melanopsin in circadian responses to light. *Science* **298,** 2211–2213 (2002).
6. Hattar, S., Liao, H. W., Takao, M., Berson, D. M. & Yau, K. W. Melanopsin-containing retinal ganglion cells: architecture, projections, and intrinsic photosensitivity. *Science* **295,** 1065–1070 (2002).
7. Panda, S. *et al.* Melanopsin is required for non-image-forming photic responses in blind mice. *Science* **301,** 525–527 (2003).
8. Thapan, K., Arendt, J. & Skene, D. J. An action spectrum for melatonin suppression: evidence for a novel non-rod, non-cone photoreceptor system in humans. *J. Physiol. (Lond.)* **535,** 261–267 (2001).
9. Provencio, I. *et al.* A novel human opsin in the inner retina. *J. Neurosci.* **20,** 600–605 (2000).
10. Brainard, G. C. *et al.* Action spectrum for melatonin regulation in humans: evidence for a novel circadian photoreceptor. *J. Neurosci.* **21,** 6405–6412 (2001).
11. Hankins, M. W. & Lucas, R. J. The primary visual pathway in humans is regulated according to long-term light exposure through the action of a nonclassical photopigment. *Curr. Biol.* **12,** 191–198 (2002).
12. Hannibal, J. *et al.* Melanopsin is expressed in PACAP-containing retinal ganglion cells of the human retinohypothalamic tract. *Invest. Ophthalmol. Vis. Sci.* **45,** 4202–4209 (2004).
13. Dacey, D., Peterson, B., Robinson, F. & Gamlin, P. Fireworks in the primate retina: *in vitro* photodynamics reveals diverse LGN-projecting ganglion cell types. *Neuron* **37,** 15–27 (2003).
14. Dacey, D. M. & Lee, B. B. The blue-ON opponent pathway in primate retina originates from a distinct bistratified ganglion cell type. *Nature* **367,** 731–735 (1994).
15. Hood, D. C. & Finkelstein, M. A. in *Handbook of Perception and Human Performance* Vol. 1 (eds Boff, K. R., Kaufman, L. & Thomas, J. P.) Ch. 5, 1–66 (John Wiley and Sons, New York, 1986).
16. Takahashi, J. S., DeCoursey, P. J., Bauman, L. & Menaker, M. Spectral sensitivity of a novel photoreceptive system mediating entrainment of mammalian circadian rhythms. *Nature* **308,** 186–188 (1984).
17. Fain, G. L., Matthews, H. R., Cornwall, M. C. & Koutalos, Y. Adaptation in vertebrate photoreceptors. *Physiol. Rev.* **81,** 117–151 (2001).
18. Mollon, J. D. & Jordan, G. Eine evolutionare Interpretation des menschlichen Farbensehens. *Die Farbe* **35/36,** 139–170 (1989).
19. Valberg, A., Lee, B. B. & Tigwell, D. A. Neurones with strong inhibitory s-cone inputs in the macaque lateral geniculate nucleus. *Vision Res.* **26,** 1061–1064 (1986).
20. Cottaris, N. & DeValois, R. Temporal dynamics of chromatic tuning in macaque primary visual cortex. *Nature* **395,** 896–900 (1998).
21. Krauskopf, J., Williams, D. R. & Heeley, D. W. Cardinal directions of color space. *Vision Res.* **22,** 1123–1131 (1982).
22. Klug, K., Herr, S., Ngo, I. T., Sterling, P. & Schein, S. Macaque retina contains an S-cone OFF midget pathway. *J. Neurosci.* **23,** 9881–9887 (2003).
23. Barlow, H. B. & Levick, W. R. Changes in the maintained discharge with adaptation level in the cat retina. *J. Physiol. (Lond.)* **202,** 699–718 (1969).
24. Marrocco, R. T. Possible neural basis of brightness magnitude estimations. *Brain Res.* **86,** 128–133 (1975).
25. Kayama, Y., Riso, R. R., Bartlett, J. R. & Doty, R. W. Luxotonic responses of units in macaque striate cortex. *J. Neurophysiol.* **42,** 1495–1517 (1979).
26. Kinoshita, M. & Komatsu, H. Neural representation of the luminance and brightness of a uniform surface in the macaque primary visual cortex. *J. Neurophysiol.* **86,** 2559–2570 (2001).
27. Barlow, R. B. Jr & Verrillo, R. T. Brightness sensation in a ganzfeld. *Vision Res.* **16,** 1291–1297 (1976).
28. Packer, O. *et al.* Characterization and use of a digital light projector for vision research. *Vision Res.* **41,** 427–439 (2001).
29. Diller, L. *et al.* L and M cone contributions to the midget and parasol ganglion cell receptive fields of macaque monkey retina. *J. Neurosci.* **24,** 1079–1088 (2004).
30. Enroth-Cugell, C., Robson, J. G., Schweitzer-Tong, D. E. & Watson, A. B. Spatio-temporal interactions in cat retinal ganglion cells showing linear spatial summation. *J. Physiol. (Lond.)* **341,** 279–307 (1983).

Acknowledgements We woud like to thank C. Curcio and the Age-Related Maculopathy Histopathology Laboratory (supported by the International Retinal Research Foundation, the National Eye Institute and the Vision Science Research Center), University of Alabama at Birmingham for the human retinae used in the immunohistochemical studies. Macaque retinae were provided by the Tissue Distribution program of the National Primate Research Center at the University of Washington. We thank O. Packer and T. Haun for technical assistance. Supported by US National Eye Institute grants to D.M.D., J.P., K.-W.Y., H.W.-L. and F.R.R., Vision Research Center Core grants to D.M.D. and P.D.G., an Alabama EyeSight Foundation award to P.D.G. and a Retina Research Foundation Paul Kayser Award to D.M.D.

Competing interests statement The authors declare that they have no competing financial interests.

Correspondence and requests for materials should be addressed to D.M.D. (dmd@u.washington.edu).

DRP-1-mediated mitochondrial fragmentation during EGL-1-induced cell death in *C. elegans*

Ravi Jagasia[1,2,3], Phillip Grote[3], Benedikt Westermann[2,4] & Barbara Conradt[3]

[1]*Max Planck Institute of Neurobiology, Am Klopferspitz 18a, D-82152 Planegg-Martinsried, Germany*
[2]*Institut für Physiologische Chemie, Universität München, D-81377 München, Germany*
[3]*Dartmouth Medical School, Department of Genetics, 7400 Remsen, Hanover, New Hampshire 03755, USA*
[4]*Zellbiologie, Universität Bayreuth, D-95440 Bayreuth, Germany*

Genetic analyses in *Caenorhabditis elegans* have been instrumental in the elucidation of the central cell-death machinery, which is conserved from *C. elegans* to mammals[1,2]. One possible difference that has emerged is the role of mitochondria. By releasing cytochrome *c*, mitochondria are involved in the activation of caspases in mammals[3,4]. However, there has previously been no evidence that mitochondria are involved in caspase activation in *C. elegans*. Here we show that mitochondria fragment in cells that normally undergo programmed cell death during *C. elegans* development. Mitochondrial fragmentation is